INTERNATIONAL JOURNAL OF ENERGY STUDIES

e-ISSN: 2717-7513 (ONLINE); homepage: https://dergipark.org.tr/en/pub/ijes

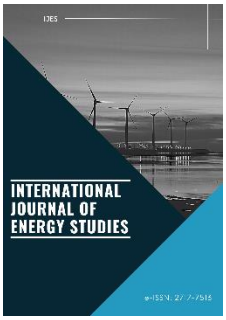

Research Article

Int J Energy Studies 2023; 8(4): 781-808

DOI: 10.58559/ijes.1327547

Received : 16 July 2023

Revised : 18 Oct 2023

Accepted : 11 Nov 2023

Energy and exergy analysis of the 1220 MW natural gas-fired Hamitabat combined cycle power plant

Göksel Topal[a], Tayfun Tanbay[b,*]

[a] *Izdemir Energy, Izmir, Türkiye, ORCID: 0000-0002-6827-9728*

[b]*Department of Mechanical Engineering, Faculty of Engineering and Natural Sciences, Bursa Technical University, Bursa, Türkiye, ORCID: 0000-0002-0428-3197*

([*]Corresponding Author: tayfun.tanbay@btu.edu.tr)

Highlights

- Energy and exergy analysis of the Hamitabat combined cycle power plant is carried out.
- Combined cycle plant has a thermal efficiency of 59.70% and an exergy efficiency of 58.52%.
- The 520 million € renovation project, completed in 2017, increased the thermal and exergy efficiencies of the plant by 13.70% and 13.52%, respectively.
- Combustion chamber causes 77.61% of the total exergy destruction and the component has an improvement potential of 67.992 MW.
- Thermal and exergy efficiencies of the plant can be improved by increasing the inlet temperatures of high- and intermediate-pressure turbines, and decreasing the pressure of condenser and high-pressure turbine.

You can cite this article as: Topal G, Tanbay T. Energy and exergy analysis of the 1220MW natural gas-fired Hamitabat combined cycle power plant. Int J Energy Studies 2023; 8(4): 781-808.

ABSTRACT

In this study, the energy and exergy analysis of the 1220 MW Hamitabat combined cycle power plant (CCPP) that was renovated in 2017 with a 520 million € project is carried out. A thermodynamic model is built by applying the conservation of mass and energy principles and operating data are obtained from the plant operators. Exergy analysis is performed with the exergy balance equation to determine the exergy efficiencies and improvement potentials of all components. Also, parametric analyses are carried out to investigate the methods to enhance the performance of the plant. The plant has thermal and exergy efficiencies of 59.70% and 58.52%, respectively and these values are 13.70% and 13.52% higher than the thermal and exergy efficiencies of the original plant, respectively. Results showed that the combustion chamber (CC) has the highest rate of exergy destruction, and it is responsible for 77.61% of the total irreversibilities. The improvement potential of the CC is found to be 67.992 MW, and the prevention of heat loss from CC can increase the thermal and exergy efficiencies of the plant by 3.88% and 3.80%, respectively. Parametric analyses showed that the plant performance can be enhanced by increasing the inlet temperatures of high- and intermediate-pressure turbines, and decreasing the pressures of condenser and high-pressure turbine.

Keywords: Combined cycle, Natural gas, Energy analysis, Exergy analysis, Improvement potential

1. INTRODUCTION

The worldwide population growth and rapid development of industrial sectors increase the demand for energy. The development and welfare levels of countries are directly related to the amount of energy consumption, however as the gross domestic product per capita increases, the efficient utilization of energy becomes important for sustainable development [1]. The effective use of energy become even more important in recent years due to the Covid-19 pandemic induced energy crisis. The rapid transition to renewable energy and the consequential decommissioning of thermal power plants due to the environmental policies made a negative contribution to the crisis. In 2022, the effects of the energy crisis have worsened with the Russia-Ukraine war that threatened European Union's climate change targets [2]. In fact, thermal power plants are being reactivated and fossil fuel-based electricity production surpassed renewables in the European Union [3].

Energy can be produced from fossil fuels, renewable sources and nuclear power plants. Although renewable resources have advantages such as being infinite, environmentally friendly and having low maintenance costs, a country's power generation infrastructure cannot solely depend on renewable energy, since these systems have a low capacity factor. Nuclear power plants have a high availability, however the public tend to have a negative perception towards nuclear energy due to the Chernobyl and Fukushima accidents, and the final repository of spent nuclear fuel is still a major concern for the nuclear industry. CCPPs combine gas and steam turbines to achieve high thermal efficiencies and therefore can produce electricity from fossil fuels economically. These plants can be operated in a flexible manner, and be adapted to different load conditions [4].

Thermodynamic modeling and analysis of CCPPs has been considered in many studies, and are useful for examining the component-based and global performance of the plant. In a review study [5], the performance optimization of CCPPs were considered. The same research group also reviewed the exergy analysis of CCPPs with different configurations in [6]. Garcia et al. [7] reviewed combined cycles that employ different energy sources and investigated the use of trilateral bottoming cycle on the thermal efficiency of CCPPs. Exergy analysis of a CCPP with reheat and closed loop steam cooled gas turbines was carried out by [8], and the simulations showed that both gas turbine (GT) types increased the performance of the plant. Sue and Chuang [9] presented an exergy analysis of a CCPP and calculated that the exergy efficiency decreased by 2.4% when the plant load is decreased from 100% to 50%. Ertesvag et al. [10] investigated the integration of an auto-thermal reformer to a CCPP with the aid of a thermodynamic analysis. The

authors found that a 200℃ increase in the GT inlet temperature (TIT) improved the thermal efficiency by 4.4% and reduced the CO_2 emission. The impact of ambient temperature on the characteristics of a CCPP was studied by [11]. A temperature range of $0-35℃$ was chosen, and the analysis revealed that the power output varied by 75 MW in the considered range.

An advanced exergoeconomic analysis of a CCPP was conducted by Cziesla et al. [12], and it was found that improving the GT section was more important than the enhancements of the bottom cycle. Thermodynamic analysis of a CCPP was performed by Sanjay et al. [13]. The study reported a thermal efficiency of 62% and revealed that the combustion chamber (CC) had the largest exergy destruction. In a closely related work, an analysis of a CCPP with an intercooled GT was presented [14]. The intercooling increased the power production by 20% and the rational efficiency by 3.13%. A constraint optimization was carried out for a triple-pressure reheat CCPP by [15], and the results indicated that the plant efficiency can be enhanced by 3.6-3.8% via increasing the TIT and reducing the heat recovery steam generator (HRSG) entropy generation. Thermodynamic analysis of a similar CCPP was presented, and the effects of condenser pressure, ambient and cooling water temperatures, plant load, pressure losses and ratio of excess air for combustion were studied by [16]. Koch et al. [17] performed an exergy and economy based optimization study to minimize the product cost of a CCPP. The analysis revealed that a double-pressure HRSG without a supplementary firing unit is the best choice for a 240 MW plant.

Exergy analysis of a CCPP was performed by [18], which showed that the plant had a thermal efficiency of 47% and an exergy efficiency of 45.55% when the duct burner is inoperative, and CC caused the largest exergy destruction. The exergoenvironmental analysis and optimization of a CCPP was conducted by [19]. It was found that increasing the TIT decreased the exergy destruction cost and lower fuel consumption reduced the emissions of CC which had the largest irreversibility. Thermoeconomic optimization of a CCPP was performed by [20] to determine the optimum design conditions that minimize the plant costs. The study also investigated the influence of power output and fuel cost on CCPP's performance. An exergetic assessment of a CCPP was made by [21], which showed that 68% of the irreversibility caused by CC is unavoidable. The impact of HRSG configuration on the exergetic and economic characteristics of a CCPP was studied by [22]. Comparison between double and triple pressure HRSGs revealed that the triple pressure configuration was thermodynamically and economically advantageous. The HRSG of a CCPP was also the subject of [23], and it was found that the plant's efficiency could be maximized

by optimizing the flue gas inlet temperature. Thermodynamic analysis of a CCPP integrated to a biomass gasification plant was presented by [24]. Compressor pressure ratio (CPR), TIT and heat-exchanger temperature difference were used in the parametric analyses to study the plant's performance.

An advanced exergoeconomic analysis of a 55 MW CCPP was presented by [25], and the results showed that the CC, HRSG, high-pressure steam turbine (HPST) and condenser had high improvement potentials. Parametric advanced exergy analysis of a CCPP was carried out by [26] which indicated that increasing the TIT and CPR improved the efficiency of the plant. The same author also carried out another advanced exergy analysis and multiobjective optimization of a CCPP to optimize emission and avoidable irreversibility of the plant simultaneously [27]. Unlike the results of [26], the optimization revealed that the CCPP's performance can be improved by increasing the CPR and decreasing TIT and duct burner mass flow rate. The use of diesel fuel instead of natural gas in a CCPP was examined by [28]. The comparative analysis indicated that natural gas yield a better performance in terms of both exergy, economy and environment. In another work, an exergoeconomic analysis of a CCPP was performed to optimize the plant performance [29]. Thermal and exergy efficiencies, investment cost and levelized cost of electricity were chosen as performance indicators. Three scenarios, in which priority was given to different objective functions, were considered, and it was found that the optimum design depended on the weights of the indicators.

A comparison of utilizing F- and H-class GT technologies of Siemens in a CCPP was given by [30]. It was found that the H-class turbine has a 2.3% higher exergy efficiency than its counterpart and the levelized cost of electricity for H-class was 0.8 $/MWh less than the F-class turbine. An exergoeconomic and environmental analysis of a CCPP utilizing a flameless burner was presented by [31]. The analysis revealed that the plant's thermal efficiency increased by 6% and its CO_2 emission decreased by 5.63% due to the use of the flameless burner. Energy-exergy analysis of a 119.2 MW [32], 180 MW [33], a 747 MW [34], a 396 MW [35], a 820 MW [36] and a 400 MW [37] CCPP revealed that the CC is the largest source of irreversibility. Thermodynamic analysis of a 1240 MW CCPP, which focused on the steam cycle, showed that the heat transfer in HRSG is the main source of irreversibility [4]. The results also revealed that the low-pressure steam turbine (LPST) outlet steam quality and superheating and reheating pressures of the HRSG had a noticeable impact on plant's performance. Pattanayak and Padhi [38] proposed a process based on

compressor precooling and fuel preheating to improve the energetic and emission characteristics of a CCPP. The analysis showed that the thermal efficiency could be enhanced by 0.58-2.2% by decreasing the air temperature from 35℃ to 20℃ at a relative humidity of 65%, and the CO_2 emission had its maximum at an ambient temperature range of 26-28℃. A thermodynamic analysis that investigated the impacts of the operating conditions of a CCPP was presented by Shireef and Ibrahim [39]. The analysis revealed that a decrease in ambient temperature, an increase in TIT and CPR enhanced the plant's thermal efficiency.

Turkey has an installed power of 105672 MW as of May, 2023 [40]. The total electricity production was recorded to be 328.7 TWh in 2022, and the contributions of different energy sources to the production are presented in Fig. 1. Natural gas plays an essential role in the generation of electricity. The country has a national energy policy of increasing the share of renewables and including nuclear in the energy mix. Turkey also aims to improve the efficiency of power plants, and to procure the efficient utilization of energy in domestic applications, industrial, agricultural and transportation sectors for mitigating greenhouse gas emissions. In this regard, the improvement of natural gas-fired power plant performance, which has 22.2% share in the energy mix, is crucial. Efficient use of natural gas would also provide a positive impact on the macroeconomics of Turkey since 98.08 % of the consumed gas is imported in 2021 [41].

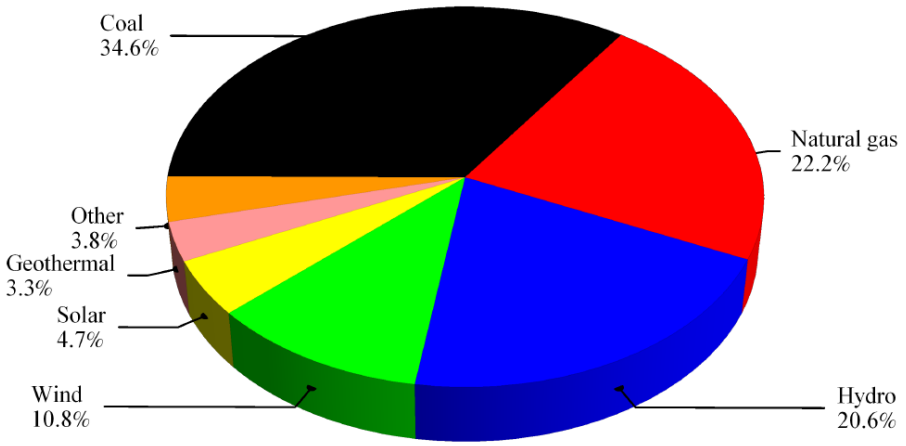

Figure 1. Contribution of different energy sources on the electricity production of Turkey [40]

Hamitabat CCPP was built in 1985 in Lüleburgaz, Kırklareli, on an area of 800000 m^2 as Turkey's first CCPP. The original plant had a capacity of 1000 MW, and it was renovated completely with a 520 million € project in 2017 to increase the plant capacity to 1220 MW. Hamitabat CCPP is a natural gas-fired plant, and consists of two units. The plant is located in a strategic position as it

connects Turkey's electricity grid to Bulgaria and Greece through the interconnected network. Hamitabat CCPP is also connected to the Turusgaz natural gas pipeline, which supplies natural gas to Turkey. The plant is crucial for the energy supply security of the Marmara region of Turkey. Cihan et al. [42] performed an energy-exergy analysis for the original version of the Hamitabat CCPP and found that the CC, GT and HRSG caused the largest exergetic losses.

In this study, the energy and exergy analysis of the renovated Hamitabat CCPP are carried out. The analysis is performed for a single unit with actual data obtained from the plant operators. The modelling of the CCPP is carried out with Mathematica 11. The novelties of the study and its contribution to the literature are as follows:

- Energy and exergy analysis of the renovated Hamitabat CCPP is carried out for the first time.
- Thermal and exergy efficiencies of the plant are determined and the heat losses/gains, exergy destruction rates and exergy efficiencies of all plant components are calculated.
- The improvement potential of plant components, which is not previously considered as a performance indicator in the analysis of CCPPs in the literature, are determined.
- The effect of combustion chamber heat loss on the performance of the plant is examined.
- Parametric analysis of the plant is made to investigate the impacts of HPST and IPST inlet temperature, and the pressure of HPST and condenser on the performance of the plant.

2. DESCRIPTION OF THE PLANT

Hamitabat CCPP has two combined cycle units. Each unit consists of a Siemens SGT5-800H H-class 400 MW GT, a Siemens SST-5000 closed-loop 210 MW steam turbine with high-, medium- and low-pressure stages and a generator. In addition, each unit contains a triple-stage HRSG, a condenser, a main cooling water system, a natural gas preheater, a gland condenser and a polishing unit. The cooling water of the plant is provided by two cooling towers having a height of 135 m, an upper diameter of 70 m and a lower diameter of 121 m.

The schematic representation of the Hamitabat CCPP is shown in Fig. 2. Electricity production from the plant is carried out through a gas and a steam cycle. In the gas cycle, air enters the compressor (C) at ambient conditions. Pressurized air then enters the CC, it reacts with preheated natural gas and the highest temperature in the cycle is obtained at the GT inlet. The combustion products expand in the GT to produce work and then enter the HRSG to transfer heat to the steam

cycle. The triple-pressure HRSG thermally couples the gas and steam cycles. Feedwater of the steam cycle enters the HRSG at state 26 and it is heated in the preheater (PH) packages to state 27. The flow is then divided to high- (state 40), intermediate- (state 30) and low-pressure (state 29) streams. The high-pressure stream is heated in the high-pressure economizer (HP ECO) to state 43. Then, the high-pressure superheater (HP SH) increases the steam temperature to the high-pressure steam turbine (HPST) inlet conditions (state 8).

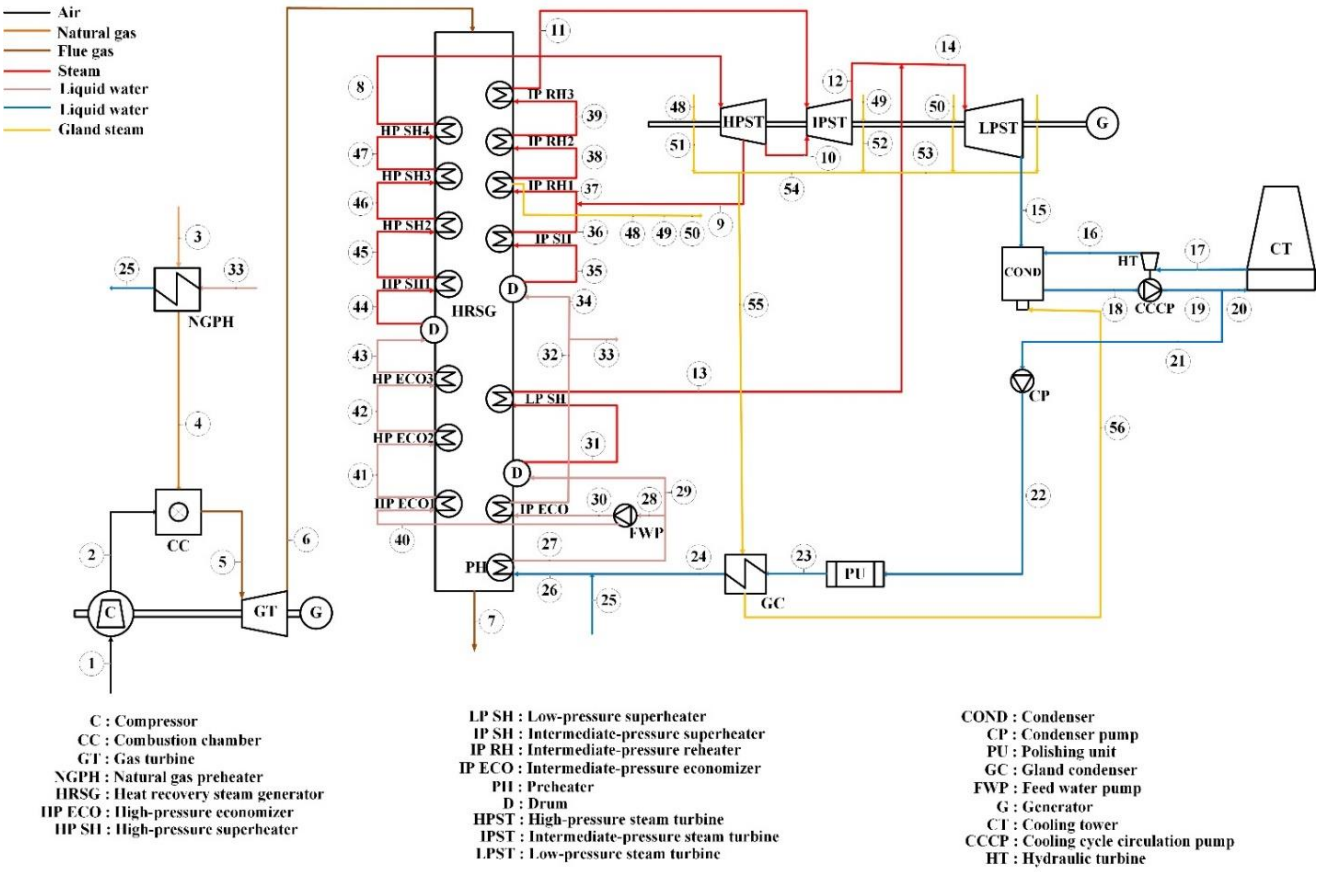

Figure 2. Schematic representation of the Hamitabat CCPP

The intermediate-pressure stream is heated in the intermediate-pressure economizer (IP ECO) and then separated at state 32 so that part of the flow is directed to the natural gas preheater (NGPH) at state 33. The remaining part of the flow at state 34 enters the intermediate-pressure drum and it is heated in the intermediate-pressure superheater (IP SH and IP RH) to the intermediate-pressure steam turbine (IPST) inlet conditions (state 11). Steam extracted from the HPST at state 9 helps the intermediate-pressure superheating process. A slight amount of steam is extracted from IP RH1 at states 48-50 for steam sealing of the steam turbines. The low-pressure stream enters the low-pressure drum and it is heated in the low-pressure superheater (LP SH) to state 13. The steam then

mixes with the outlet flow of IPST and enters the low-pressure steam turbine (LPST) at state 14. The steam turbines produce work with the expansion of the steam. The mechanical works of both gas and steam turbines are converted to electrical work with a generator. The expanded steam at the LPST outlet enters a direct contact condenser (COND) and mixes with the water circulating in the cooling cycle which is a Heller system. Water is pumped to the cooling tower (CT) with a cooling cycle circulation pump (CCCP). The power needed by the CCCP is partially supplied by the hydraulic turbine (HT) which decreases the pressure of water to LPST outlet pressure. Flow is separated at the outlet of the CCCP where majority of water is directed to CT and the rest of the stream is pumped with the condenser pump (CP) to a polishing unit (PU) where harmful gases and substances are removed from the cycle. Steam extracted at states 48-50 is directed to gland condenser (GC) and then mixes with the main stream.

3. PERFORMANCE ANALYSIS

The main assumptions for the energy-exergy analysis of the Hamitabat CCPP are:

- All processes are steady-flow.
- Turbines, pumps and compressors are adiabatic.
- Natural gas is composed volumetrically of 97.1874% methane (CH_4), 1.5719% ethane (C_2H_6), 0.4939% propane (C_3H_8) and 0.7468% nitrogen (N_2).
- Air consists of 79% N_2 and 21% oxygen (O_2).
- JANAF database [43] is utilized for the thermophysical data of water, constituents of air and combustion products, and CH_4, while data of [44] and [45] are used for C_2H_6 and C_3H_8, respectively.
- The temperature dependence of the specific heats of natural gas, air and combustion products are considered in calculations. The enthalpy change of these gases are calculated as

$$\Delta\bar{h}_i(T_j) = \int_{T_{ref}}^{T_j} \bar{c}_{p,i}(T)dT\,, \quad i = CH_4, C_2H_6, C_3H_8, N_2, O_2, CO_2, H_2O \tag{1}$$

where T is temperature and $\bar{h}$ and $\bar{c}_p$ are molar enthalpy and specific heat, respectively. Specific heats of all species are interpolated with third order polynomials to construct the $\bar{c}_{p,i}(T)$ relationships and integrations are carried out analytically.

- Inlet conditions of C represent the dead state conditions.

- The reference temperature and pressure used for the analysis of the CC are $T_{ref} = 25℃$ and $P_{ref} = 1atm$, respectively.

3.1. Energy Analysis

Energy analysis of the CCPP is performed by applying the conservation of energy and conservation of mass in steady-state form to the components of the plant

$$\sum \dot{m}_{in} = \sum \dot{m}_{out} \tag{2}$$

$$\dot{Q}_{in} + \dot{W}_{in} + \sum (\dot{m}h)_{in} = \dot{Q}_{out} + \dot{W}_{out} + \sum (\dot{m}h)_{out} \tag{3}$$

where $\dot{m}$, $\dot{Q}$ and $\dot{W}$ are the mass flow, heat transfer and work transfer rates, respectively, and h is the enthalpy. For the analysis of the CC, Eq. (3) should be modified to take into account the chemical reactions. The CC does not involve any work transfer, and therefore the steady-state energy conservation equation for a chemically reacting system can be expressed as

$$\dot{Q}_{in} + \sum \dot{n}_r \left(\bar{h}_f^0 + \bar{h} - \bar{h}^0\right)_r = \dot{Q}_{out} + \sum \dot{n}_p \left(\bar{h}_f^0 + \bar{h} - \bar{h}^0\right)_p \tag{4}$$

where $\dot{n}$ is the molar flow rate and $\bar{h}_f^0$ is the formation enthalpy at a reference temperature and pressure of a chemical specie. The subscripts r and p denote reactants and products, respectively. Since actual plant data is obtained from the operators, Eq. (3) can be used to calculate power production of gas and steam turbines, power consumption of compressor and pumps, heat rejection rate of CT, heat gain or loss rates of HRSG, COND, PU, GC, NGPH and flow mixing/separation, while Eq. (4) can be used to determine the heat loss rate of CC. The expressions are presented in Table 1.

Table 1. Energy and exergy analysis of the Hamitabat CCPP components

Component	Energy and exergy analysis
C	$\dot{W}_C = \dot{m}_2(h_2 - h_1)$ $\dot{X}_{dest,C} = \dot{X}_1 - \dot{X}_2 + \dot{W}_C$
CC	$\dot{Q}_{CC} = \dot{Q}_{LHV} + \sum_{j\in air} \dot{n}_j \Delta\bar{h}_j(T_2) + \sum_{j\in ng} \dot{n}_j \Delta\bar{h}_j(T_4) - \sum_{j\in flue} \dot{n}_j \Delta\bar{h}_j(T_5)$ $\dot{X}_{dest,CC} = \dot{X}_2 + \dot{X}_4 - \dot{X}_5 - \left(1 - \frac{T_0}{T_5}\right)\dot{Q}_{CC} + \dot{X}_{fuel}$ $air \rightarrow N_2, O_2 \qquad ng \rightarrow CH_4, C_2H_6, C_3H_8, N_{2f} \qquad flue \rightarrow CO_2, H_2O, N_2, O_2$
GT	$\dot{W}_{GT} = \dot{m}_5(h_5 - h_6)$ $\dot{X}_{dest,GT} = \dot{X}_5 - \dot{X}_6 - \dot{W}_{GT}$
NGPH	$\dot{Q}_{NGPH} = \dot{m}_3 h_3 + \dot{m}_{33} h_{33} - (\dot{m}_4 h_4 + \dot{m}_{25} h_{25})$ $\dot{X}_{dest,NGPH} = \dot{X}_3 + \dot{X}_{33} - (\dot{X}_4 + \dot{X}_{25}) - \left(1 - \frac{T_0}{T_{ave}}\right)\dot{Q}_{NGPH}$
HRSG	$\dot{Q}_{HRSG} = \dot{m}_6 h_6 + \dot{m}_{26} h_{26} + \dot{m}_{29} h_{29} + \dot{m}_{30} h_{30} + \dot{m}_{34} h_{34} + \dot{m}_{37} h_{37} + \dot{m}_{40} h_{40} - (\dot{m}_7 h_7 + \dot{m}_8 h_8 + \dot{m}_{11} h_{11} + \dot{m}_{13} h_{13} + \dot{m}_{27} h_{27} + \dot{m}_{32} h_{32} + \dot{m}_{36} h_{36} + \dot{m}_{48} h_{48} + \dot{m}_{49} h_{49} + \dot{m}_{50} h_{50})$ $\dot{X}_{dest,HRSG} = \underbrace{\dot{X}_6 + \dot{X}_{26} + \dot{X}_{29} + \dot{X}_{30} + \dot{X}_{34} + \dot{X}_{37} + \dot{X}_{40}}_{\dot{X}_{mass\ in,HRSG}} - \underbrace{\left(1 - \frac{T_0}{T_{ave}}\right)\dot{Q}_{HRSG}}_{\dot{X}_{heat\ out,HRSG}} - \underbrace{(\dot{X}_7 + \dot{X}_8 + \dot{X}_{11} + \dot{X}_{13} + \dot{X}_{27} + \dot{X}_{32} + \dot{X}_{36} + \dot{X}_{48} + \dot{X}_{49} + \dot{X}_{50})}_{\dot{X}_{mass\ out,HRSG}}$
HPST	$\dot{W}_{HPST} = \dot{m}_8 h_8 - (\dot{m}_9 h_9 + \dot{m}_{10} h_{10})$ $\dot{X}_{dest,HPST} = \dot{X}_8 - (\dot{X}_9 + \dot{X}_{10}) - \dot{W}_{HPST}$
IPST	$\dot{W}_{IPST} = \dot{m}_{10} h_{10} + \dot{m}_{11} h_{11} - \dot{m}_{12} h_{12}$ $\dot{X}_{dest,IPST} = \dot{X}_{10} + \dot{X}_{11} - \dot{X}_{12} - \dot{W}_{IPST}$
LPST	$\dot{W}_{LPST} = \dot{m}_{14}(h_{14} - h_{15})$ $\dot{X}_{dest,LPST} = \dot{X}_{14} - \dot{X}_{15} - \dot{W}_{LPST}$
COND	$\dot{Q}_{COND} = \dot{m}_{15} h_{15} + \dot{m}_{16} h_{16} + \dot{m}_{56} h_{56} - \dot{m}_{18} h_{18}$ $\dot{X}_{dest,COND} = \dot{X}_{15} + \dot{X}_{16} + \dot{X}_{56} - \dot{X}_{18} - \left(1 - \frac{T_0}{T_{ave}}\right)\dot{Q}_{COND}$
HT	$\dot{W}_{HT} = \dot{m}_{17}(h_{17} - h_{16})$ $\dot{X}_{dest,HT} = \dot{X}_{17} - \dot{X}_{16} - \dot{W}_{HT}$
CT	$\dot{Q}_{CT,cooling} = \dot{m}_{20}(h_{20} - h_{17})$ $\dot{X}_{dest,CT} = \dot{X}_{20} - \dot{X}_{17} - \left(1 - \frac{T_0}{T_{ave}}\right)\dot{Q}_{CT,cooling}$
CCCP	$\dot{W}_{CCCP} = \dot{m}_{18}(h_{19} - h_{18})$ $\dot{X}_{dest,CCCP} = \dot{X}_{18} - \dot{X}_{19} + \dot{W}_{CCCP}$
CP	$\dot{W}_{CP} = \dot{m}_{22}(h_{22} - h_{21})$ $\dot{X}_{dest,CP} = \dot{X}_{21} - \dot{X}_{22} + \dot{W}_{CP}$
PU	$\dot{Q}_{PU} = \dot{m}_{22}(h_{22} - h_{23})$

	$\dot{X}_{dest,PU} = \dot{X}_{22} - \dot{X}_{23} - \left(1 - \frac{T_0}{T_{ave}}\right)\dot{Q}_{PU}$
GC	$\dot{Q}_{GC} = \dot{m}_{23}h_{23} + \dot{m}_{55}h_{55} - (\dot{m}_{24}h_{24} + \dot{m}_{56}h_{56})$
	$\dot{X}_{dest,GC} = \dot{X}_{23} + \dot{X}_{55} - (\dot{X}_{24} + \dot{X}_{56}) - \left(1 - \frac{T_0}{T_{ave}}\right)\dot{Q}_{GC}$
FWP	$\dot{W}_{FWP} = \dot{m}_{30}h_{30} + \dot{m}_{40}h_{40} - \dot{m}_{28}h_{28}$
	$\dot{X}_{dest,FWP} = \dot{X}_{28} - (\dot{X}_{30} + \dot{X}_{40}) + \dot{W}_{FWP}$
Mixing or separation	$\dot{Q} = \sum(\dot{m}h)_{in} - \sum(\dot{m}h)_{out}$
	$\dot{X}_{dest} = \sum \dot{X}_{in} - \sum \dot{X}_{out} - \left(1 - \frac{T_0}{T_{ave}}\right)\dot{Q}$

Thermal efficiency of the Hamitabat CCPP is determined by

$$\eta_{th} = \frac{\dot{W}_{net}}{\dot{Q}_{LHV}} \tag{5}$$

where $\dot{W}_{net}$ is the net power production rate and $\dot{Q}_{LHV}$ represents the energy transferred to the plant as a result of the combustion reaction in the CC, and it is related to the molar flow rates of air and fuel and to the lower heating value of the fuel through the formation enthalpies of chemical species:

$$\dot{W}_{net} = \dot{W}_{GT} + \dot{W}_{HPST} + \dot{W}_{IPST} + \dot{W}_{LPST} + \dot{W}_{HT} - \left(\dot{W}_C + \dot{W}_{CP} + \dot{W}_{FWP} + \dot{W}_{CCCP}\right) \tag{6}$$

$$\dot{Q}_{LHV} = \sum_r \dot{n}_{r,4}\,\bar{h}^{\circ}_{f,r} - \sum_p \dot{n}_{p,5}\,\bar{h}^{\circ}_{f,p}, \quad r = CH_4, C_2H_6, C_3H_8, \quad p = CO_2, H_2O \tag{7}$$

3.2. Exergy Analysis

Irreversibilities of CCPP components can be calculated by using the steady-state exergy balance equation:

$$\dot{X}_{dest} = \sum_{i\in in} \dot{X}_i - \sum_{i\in out} \dot{X}_i + \left(1 - \frac{T_0}{T_b}\right)\dot{Q}_{in} - \left(1 - \frac{T_0}{T_b}\right)\dot{Q}_{out} + \dot{W}_{in} - \dot{W}_{out} \tag{8}$$

In Eq. (8), T_0 is the dead state temperature, T_b is the boundary temperature at which heat is transferred and the exergy flow rate is defined by

$$\dot{X}_i = \dot{m}_i[h_i - h_0 - T_0(s_i - s_0)] \quad (9)$$

where subscript 0 denotes dead state properties. Enthalpies and entropies of air, natural gas and flue gas are calculated by

$$h = \frac{\sum_j y_j \bar{h}_j}{M_m}, \quad s = \frac{\sum_j y_j \bar{s}_j}{M_m}, \quad j \rightarrow \begin{cases} N_2, O_2, & m = \text{air} \\ CH_4, C_2H_6, C_3H_8, N_2, & m = \text{natural gas} \\ CO_2, H_2O, N_2, O_2, & m = \text{flue gas} \end{cases} \quad (10)$$

where y_j and $\bar{s}_j$ are the molar fraction and entropy of j[th] specie, respectively, and M is the molar mass.

Exergy efficiency of a thermodynamic process is defined as [46]

$$\eta_{ex} = \frac{\dot{X}_{rec}}{\dot{X}_{exp}} = 1 - \frac{\dot{X}_{dest}}{\dot{X}_{exp}} \quad (11)$$

where $\dot{X}_{rec}$ and $\dot{X}_{exp}$ are the recovered and expended exergy rates, respectively. The mass flow rate-averaged surface temperatures of plant components that are used to calculate the exergy transfer by heat are defined as

$$T_{ave} = \frac{\sum_i \dot{m}_i T_i}{\sum_i \dot{m}_i} \quad (12)$$

Exergy efficiency of the CCPP is determined by:

$$\eta_{ex} = \frac{\dot{W}_{net}}{\dot{X}_{fuel}} \quad (13)$$

Exergy of the fuel is calculated by utilizing the Gibbs function of formations for the reactants and products. In explicit form

$$\dot{X}_{fuel} = \sum_r \dot{n}_r \left\{ h^0_{f,r} + \Delta\bar{h}_r(T_0) - T_0 \left[\bar{s}_r(T_1, P_{ref}) - R_u \ln\left(y_r \frac{P_0}{P_{ref}} \right) \right] \right\} - \sum_p \dot{n}_p \left\{ h^0_{f,p} + \Delta\bar{h}_p(T_0) - T_0 \left[\bar{s}_p(T_1, P_{ref}) - R_u \ln\left(y_p \frac{P_0}{P_{ref}} \right) \right] \right\} \quad (14)$$

where R_u is the universal gas constant.

The improvement potential was defined by Van Gool [47] as

$$I_p = \left(1 - \frac{\dot{X}_{out}}{\dot{X}_{in}}\right)\left(\dot{X}_{in} - \dot{X}_{out}\right) \quad (15)$$

where $\dot{X}_{in}$ and $\dot{X}_{out}$ represent incoming and outgoing total exergy transfer rate, respectively by heat, work and mass transfer. By using Eq. (8), the improvement potential can also be expressed as:

$$I_p = \frac{\dot{X}^2_{dest}}{\dot{X}_{in}} \quad (16)$$

4. RESULTS AND DISCUSSION

Table 2 presents the temperature, pressure and mass flow rate data obtained from the plant operators and the corresponding enthalpy, entropy and exergy flow rates of all thermodynamic states for a single unit of the plant. The conditions of the flue gas are determined by the volumetric compositions of air and natural gas given in Section 3, which lead to the following combustion reaction in the CC expressed in terms of molar flow rates as

$$1.22759\ CH_4 + 0.019855\ C_2H_6 + 0.00623874\ C_3H_8 + 22.753\ N_2 + 6.04882\ O_2 \rightarrow 1.28602\ CO_2 + 2.5397\ H_2O + 22.753\ N_2 + 3.49295\ O_2 \quad (17)$$

Table 2. Thermodynamic conditions for the states of Hamitabat CCPP

State	Fluid	T(℃)	$P(MPa)$	$\dot{m}(kg/s)$	$h(kJ/kg)$	$s(kJ/kg \cdot K)$	$\dot{X}(kW)$
1	Air	14.8	0.0992	830.680	256.94	6.8608	0.000
2	Air	423.0	1.6800	830.680	680.93	6.9560	329.410
3	Natural gas	15.0	3.7800	20.830	522.08	9.5460	11.009

4	Natural gas	215.0	3.7800	20.830	1014.37	10.8252	13.591
5	Flue gas	1336.0	1.5600	851.510	1849.86	8.2377	1058.830
6	Flue gas	631.9	0.1021	851.510	956.30	8.3102	280.172
7	Flue gas	87.9	0.1021	851.510	343.24	7.2853	9.445
8	Steam	610.0	16.8000	108.654	3593.20	6.6431	182.743
9	Steam	371.8	3.7330	102.482	3151.07	6.7044	125.242
10	Steam	371.0	3.7000	6.172	3149.95	6.7065	7.532
11	Steam	573.0	3.7000	117.629	3615.50	7.3345	177.042
12	Steam	295.0	0.5000	123.801	3054.24	7.4425	112.996
13	Steam	241.1	0.4820	15.000	2942.90	7.2543	12.834
14	Steam	290.0	0.4950	138.801	3044.01	7.4289	125.809
15	Steam	37.1	0.0063	138.801	2353.70	7.6225	22.258
16	Water	30.0	0.0063	9000.000	125.73	0.4367	13.679
17	Water	30.0	0.1700	9000.000	125.89	0.4367	15.227
18	Water	36.0	0.0063	9140.301	150.82	0.5186	27.896
19	Water	36.02	0.3800	9140.301	151.23	0.5187	31.294
20	Water	36.02	0.3800	9000.000	151.23	0.5187	30.814
21	Water	36.02	0.3800	140.301	151.23	0.5187	0.480
22	Water	37.1	2.8520	140.301	157.95	0.5323	0.872
23	Water	36.6	2.8020	140.301	155.82	0.5256	0.844
24	Water	38.7	2.7520	140.301	164.54	0.5539	0.926
25	Water	42.0	4.0000	14.330	179.41	0.5973	0.129
26	Water	39.1	2.8520	154.631	166.29	0.5592	1.055
27	Water	151.6	2.1920	154.631	640.13	1.8561	16.582
28	Water	151.6	2.1920	139.631	640.13	1.8561	14.973
29	Water	151.6	2.1920	15.000	640.13	1.8561	1.608
30	Water	152.3	4.1130	30.977	644.32	1.8610	3.408
31	Steam	153.3	0.5190	15.000	2749.82	6.8077	11.866
32	Water	241.6	4.0740	30.977	1045.33	2.7152	8.210
33	Water	241.6	4.0740	14.330	1045.33	2.7152	3.798
34	Water	241.6	4.0740	16.647	1045.33	2.7152	4.412
35	Steam	246.9	3.7710	16.647	2801.81	6.0939	17.457
36	Steam	365.0	3.6860	16.647	3136.07	6.6867	20.179
37	Steam	370.0	3.7200	119.129	3147.12	6.6998	145.273
38	Steam	559.2	3.6370	117.629	3584.64	7.3045	174.426
39	Steam	589.1	3.6130	117.629	3653.05	7.3906	179.557
40	Water	156.3	18.3880	108.654	670.26	1.8854	14.008
41	Water	245.3	18.3040	108.654	1064.48	2.7186	30.774
42	Water	336.3	18.1730	108.654	1552.91	3.5825	56.814
43	Water	355.2	17.9300	108.654	1713.54	3.8422	66.141
44	Steam	356.7	17.9300	108.654	2512.69	5.1113	113.266
45	Steam	407.0	17.8550	108.654	2919.52	5.7392	137.825
46	Steam	508.8	17.7340	108.654	3299.23	6.2657	162.610
47	Steam	579.1	17.6200	108.654	3502.43	6.5169	176.828

48	Steam	300.0	0.0035	0.500	3076.91	9.4037	0.185
49	Steam	298.0	0.0035	0.500	3072.94	9.3965	0.184
50	Steam	296.0	0.0035	0.500	3068.98	9.3892	0.183
51	Steam	300.0	0.0035	0.500	3076.91	9.4037	0.185
52	Steam	298.0	0.0035	0.500	3072.94	9.3965	0.184
53	Steam	296.0	0.0035	0.500	3068.98	9.3892	0.183
54	Steam	297.0	0.0035	1.000	3070.96	9.3928	0.368
55	Steam	298.0	0.0035	1.500	3072.94	9.3965	0.553
56	Steam	45.0	0.0020	1.500	2583.47	8.2973	0.294

4.1. Performance of the Plant

Table 3 presents the results of the energy and exergy analysis of the Hamitabat CCCP. It was found by [42] that the original version of the plant had a thermal efficiency of 46% and an exergy efficiency of 45%. The efficiency values given in Table 3 show that the thermal and exergy efficiencies of the Hamitabat CCPP have improved by 13.70% and 13.52%, respectively, as a result of the 520 million € renovation project. The calculated net power output is close to the rated power of 610 MW, which is the power of a single unit. The air cycle produces a net power of 406.682 MW, and the LPST makes the largest contribution to power production in the steam cycle. The energy analysis of non-adiabatic plant components reveal that significant heat losses occur at the CC and COND.

Table 3. Main performance indicators of the Hamitabat CCPP

Power production and consumption (MW)		Heat loss (+) or gain (-) of plant components (MW)		Overall performance indicators	
$\dot{W}_{GT}$	760.877	$\dot{Q}_{CC}$	39.820	η_{th}	59.70%
$\dot{W}_{HPST}$	48.046	$\dot{Q}_{NGPH}$	2.154	η_{ex}	58.52%
$\dot{W}_{IPST}$	66.611	$\dot{Q}_{HRSG}$	-5.588	$\dot{W}_{net}$	612.511 MW
$\dot{W}_{LPST}$	95.814	$\dot{Q}_{COND}$	83.522	$\dot{Q}_{LHV}$	1026.010 MW
$\dot{W}_{HT}$	1.437	$\dot{Q}_{PU}$	0.299	$\dot{Q}_{CT,cooling}$	228.128 MW
$\dot{W}_{C}$	352.195	$\dot{Q}_{GC}$	-0.489	$\dot{X}_{fuel}$	1046.690 MW
$\dot{W}_{CCCP}$	3.734	$\dot{Q}_{mix-sep}$	-0.086	$\dot{X}_{dest,total}$	396.084 MW
$\dot{W}_{CP}$	0.942			$I_{p,total}$	72.567 MW
$\dot{W}_{FWP}$	3.404				

The exergy destruction rates, exergy efficiencies and improvement potentials of the CCPP components are presented in Table 4, and also the relative contributions of components on the total exergy destruction rate of the plant are illustrated in Fig 3. CC has the highest exergy destruction

rate and it is responsible for 77.61% of the total irreversibility. In relation to this high irreversibility, CC has a large improvement potential which corresponds to 93.70% of the total potential. HRSG, C, GT and LPST have also notable exergy destruction rates and have a total improvement potential of 3.661 MW. As for the exergy efficiencies, it is found that the GC, CP and CC have the lowest efficiencies.

Table 4. Exergy destruction rates, exergy efficiencies and improvement potentials of Hamitabat CCPP components

Component	$\dot{X}_{dest}\ (MW)$	$I_p\ (MW)$	η_{ex}
C	22.785	1.474	0.935
CC	307.389	67.992	0.706
GT	17.784	0.299	0.977
NGPH	0.488	0.0161	0.867
HRSG	25.287	1.412	0.907
HPST	1.922	0.020	0.961
IPST	4.967	0.134	0.931
LPST	7.737	0.476	0.925
COND	3.355	0.311	0.907
HT	0.111	0.001	0.928
CT	2.018	0.132	0.870
CCCP	0.336	0.004	0.910
CP	0.550	0.213	0.416
PU	0.007	0.0001	-
GC	0.214	0.033	0.173
FWP	0.961	0.050	0.718
Mix-Sep	0.173	0.0002	-

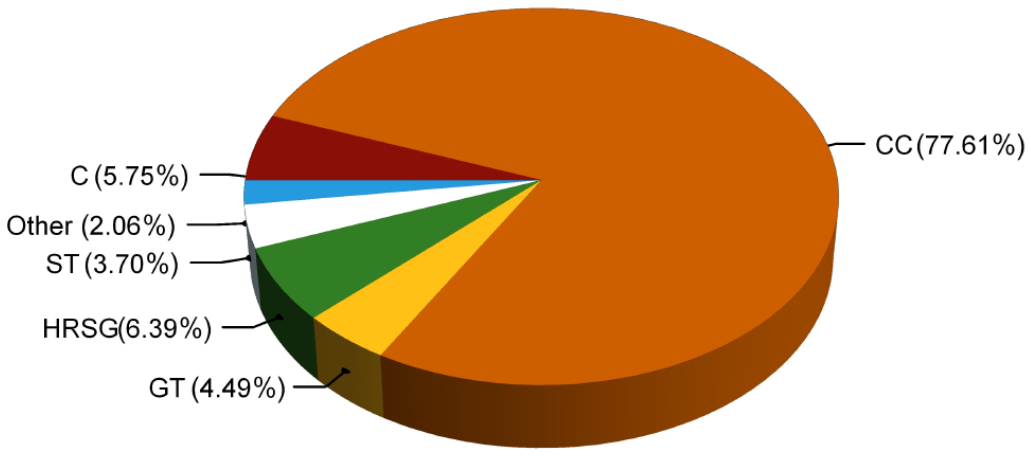

Figure 3. Exergy destruction percentages of Hamitabat CCPP components

The performance of the Hamitabat CCPP is compared with other plants for which an energy-exergy analysis is presented in the literature. Table 5 shows the thermal efficiency, exergy efficiency, and the contributions of three equipment to total exergy destruction rate that have the highest irreversibility rates. Hamitabat CCPP has the best energetic and exergetic performance among the seven plants. Componentwise comparison of the results indicate that CC is always the dominant source of irreversibility, however the second and third contributors vary from one plant to another. HRSG and GT are the second largest sources of irreversibility, while ST, COND and C are found to have the third highest exergy destruction rate. It should also be noted that, as compared to the other plants in Table 5, GT has a relatively low contribution of 4.49% and 2% [37] to $\dot{X}_{dest}$ for Hamitabat and KOSPO CCPP, respectively. This distinction between the component-based exergy destruction rates of Hamitabat-KOSPO and other CCPPs can be explained as follows. Energy-exergy analysis presented in [32-34] do not consider heat losses or gains of plant components, while in the analyses of [35] and [36] it is assumed that 2% of the heat is lost from the CC and the other components are treated as adiabatic. Among [32-37], the only energy-exergy analysis that takes into account heat transfer from all components of the plant, and therefore similar to the analysis presented in this paper, is that of [37].

Table 5. Comparison of Hamitabat CCPP's performance with six different plants.

CCPP	Nominal power (MW)	η_{th}	η_{ex}	Contribution to $\dot{X}_{dest}$ - Component (%)		
				1	2	3
ATAER [32]	119.2	45	24	CC (63)	GT (16)	ST (8)
Garri 2 [33]	180	38	49	CC (63)	GT (13.6)	ST (6.4)
Guddu [34]	747	59.12	58.24	CC (70)	HRSG (9)	GT (7)
Malay [35]	396	55.5	-	CC (75.20)	HRSG (11.30)	GT (7.97)
Brazilian [36]	826	51.54	49.32	CC (70.24)	GT (10.75)	HRSG (7.37)
KOSPO [37]	400	38	37	CC (67)	HRSG (14)	COND (7)
Hamitabat	1220	59.70	58.52	CC (77.61)	HRSG (6.39)	C (5.75)

The performance of a CCPP is highly sensitive to the CC outlet temperature since it is the maximum temperature observed in the cycle. The change in the chemical composition due to combustion and heat loss from chamber wall lead to a high level of irreversibility in the component. In order to evaluate the impact of CC heat loss on Hamitabat CCPP's performance, Eq. (4) is solved again by assuming an adiabatic combustion process. The air and natural gas inlet conditions yield an adiabatic flame temperature of $T_{5,a} = 1644.45\,K$ that is $35.3\,K$ higher than

the actual TIT. Carrying out the energy-exergy analysis with $T_{5,a}$ shows that the performance of the plant would improve significantly when the CC is adiabatic. As seen in Fig. 4, the use of the adiabatic flame temperature instead of T_5 increases thermal and exergy efficiencies by 3.88% and 3.80%, respectively. The prevention of CC heat loss also decreases the CC exergy destruction rate by 16.353 MW.

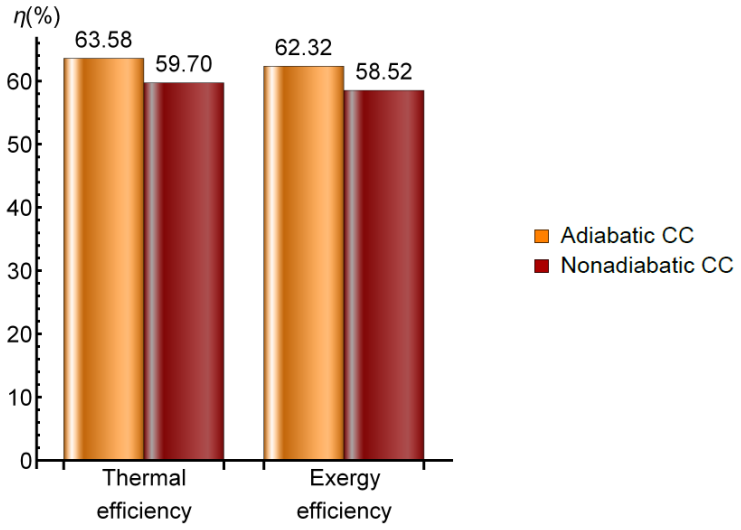

Figure 4. Effect of CC heat loss on the thermal and exergy efficiencies of the Hamitabat CCPP

4.2. Parametric Analysis

The effects of HPST and IPST inlet temperature and pressure of COND and HPST on plant's performance are examined in this section to investigate the potential improvements of the plant. The influence of COND pressure on the power production and exergy destruction rate of LPST, and on the thermal and exergy efficiencies of the Hamitabat CCPP is illustrated in Fig. 5. It is observed that decreasing the condenser pressure improves all performance indicators. The power production of the LPST increases by 3.2 MW, and the irreversibility rate decreases by 0.35 MW, while the thermal and exergy efficiencies of the CCPP improve by 0.312% and 0.306% respectively, when P_{15} is decreased by $1.2kPa$ from $6.5kPa$ to $5.3kPa$. The results indicate that although $\dot{X}_{d,LPST}$ decreases, η_{ex} tends to increase with P_{15}. This conflicting behavior can be understood by comparing the curves in Fig. 5a, which show that $\dot{W}_{LPST}$ is more sensitive to P_{15} than $\dot{X}_{d,LPST}$. The power production of the LPST increases faster than the rate of increase in $\dot{X}_{d,LPST}$. It should also be noted that, despite its negative impact on η_{th} and η_{ex}, increasing the condenser pressure increases the steam quality at the LPST outlet from 0.9057 to 0.9122, and therefore, it has a positive impact on the service life of the turbine.

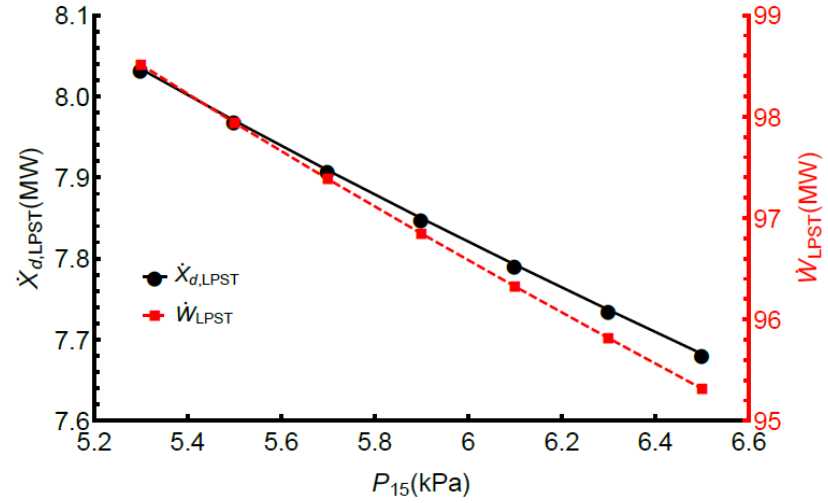

(a)

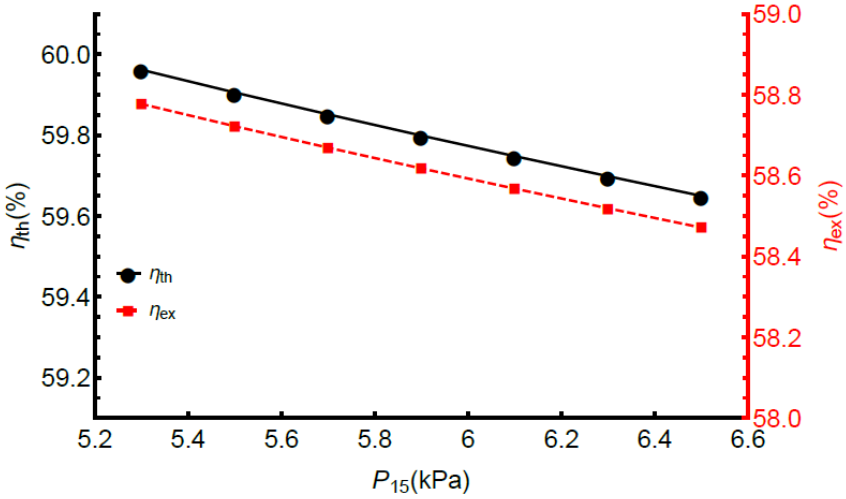

(b)

Figure 5. Variation of (a) $\dot{W}_{LPST}$, $\dot{X}_{d,LPST}$ and (b) η_{th}, η_{ex} with condenser pressure

Fig. 6 presents the impact of HPST inlet temperature on the total power production of steam turbines, irreversibility of the HPST and the thermal and exergy efficiencies of the CCPP. Increasing T_8 by 30℃ from 592℃ to 622℃ leads to an increase of 8.6 MW in $\dot{W}_{ST}$ and a decrease of 2.8 MW in $\dot{X}_{d,HPST}$. These trends have a positive impact on η_{th} and η_{ex} of the plant. The thermal and exergy efficiencies of the Hamitabat CCPP improve by %0.84 and %0.82, respectively as a result of the 30℃ increase in T_8. Also, a comparison of the curves presented in Figs. 5a and 5b reveals that the HPST inlet temperature has a larger impact on plant's performance than the condenser pressure.

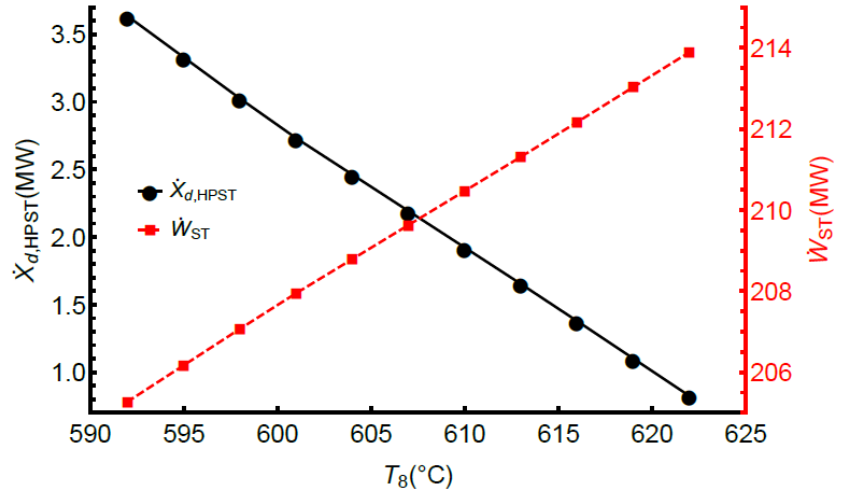

(a)

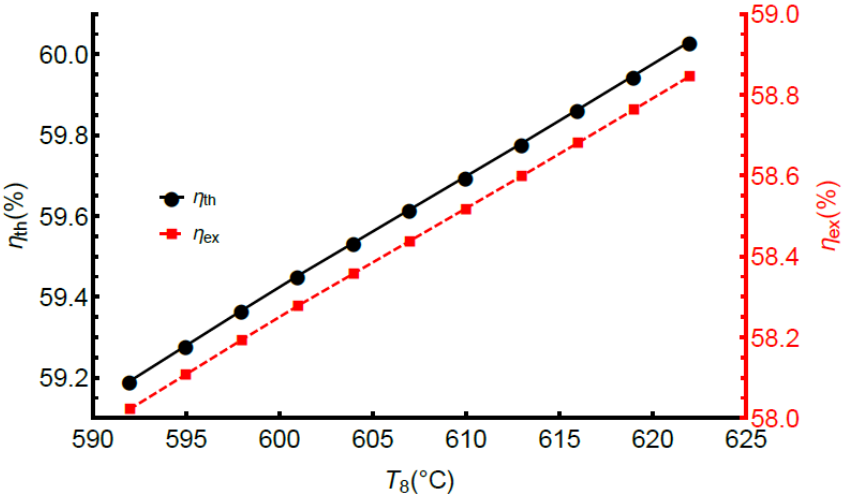

(b)

Figure 6. The impact of HPST inlet temperature on (a) $\dot{W}_{ST}$, $\dot{X}_{d,HPST}$ and (b) η_{th}, η_{ex} of CCPP

Pressure of the high-pressure stream has also an effect on Hamitabat CCPP's performance. The variations of total steam turbine power production, exergy destruction rate of HPST, and the thermal and exergy efficiencies of the plant with the pressure of the high-pressure stream are presented in Fig. 7. Increasing the HPST pressure by $2.7MPa$ decreases $\dot{W}_{ST}$ by $2.3MW$ and increases $\dot{X}_{d,HPST}$ by $2.7MW$. Therefore, as illustrated in Fig. 7a, the thermal and exergy efficiencies of the CCPP tend to deteriorate with increasing HPST pressure. In addition, the rates of variation of η_{th}, η_{ex} with HPST inlet temperature and HPST pressure shown in Figs. 6b and 7b indicate that the plant performance is more sensitive to HPST inlet temperature than it does to HPST pressure.

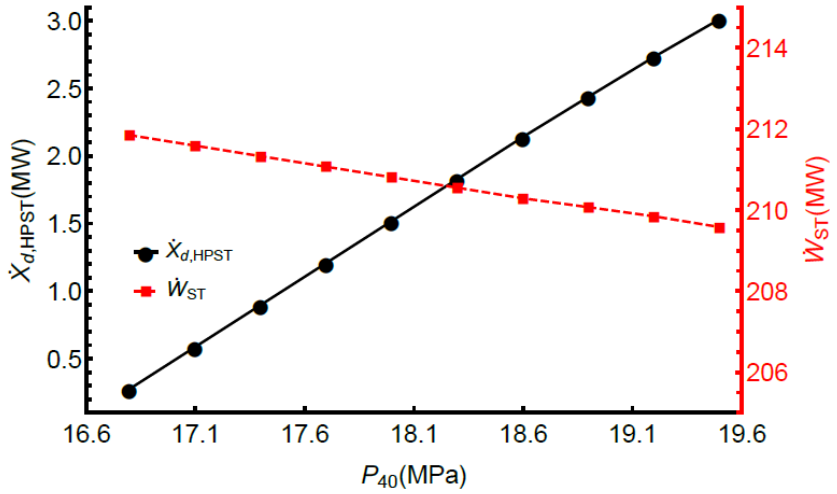

(a)

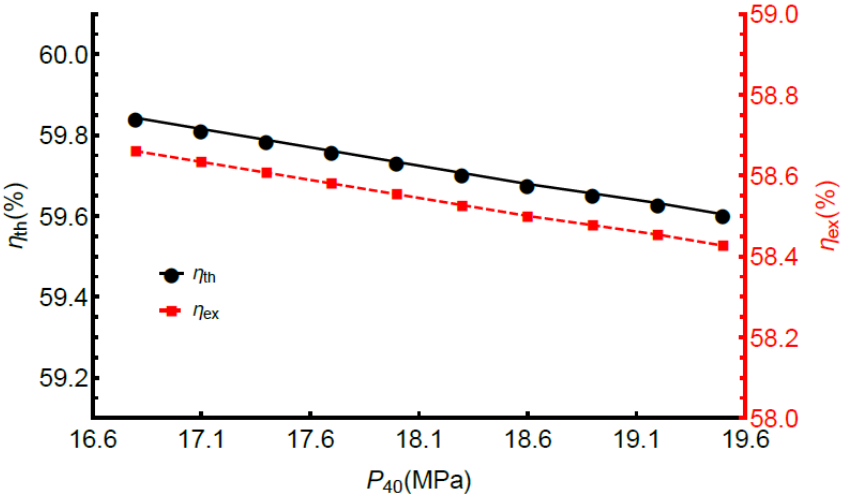

(b)

Figure 7. The effect of HPST pressure on (a) $\dot{W}_{ST}$, $\dot{X}_{d,HPST}$ and (b) η_{th}, η_{ex} of CCPP

Finally, the impact of IPST inlet temperature on the performance of steam turbines and CCPP is shown in Fig. 8. Higher IPST inlet temperature is advantageous when the energy-exergy performance of the plant is considered. The power production of steam turbines increases by 8.1MW, and the irreversibility rate of IPST decreases by 2.8 MW as a result of a 30℃ increment in T_{11}. The improvements in $\dot{W}_{ST}$ and $\dot{X}_{d,IPST}$ lead to an increase of 0.79% and 0.77% in η_{th} and η_{ex} of the Hamitabat CCPP, respectively.

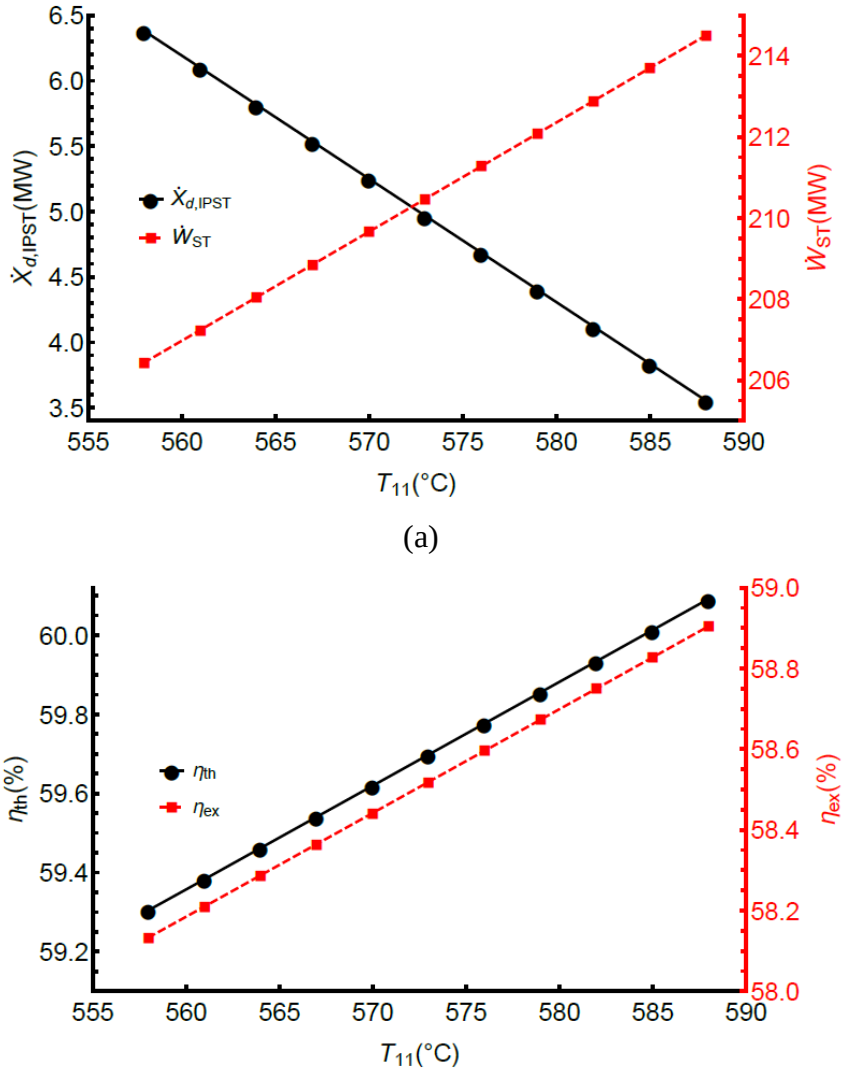

Figure 8. Variation of (a) $\dot{W}_{ST}$, $\dot{X}_{d,IPST}$ and (b) η_{th}, η_{ex} with IPST inlet temperature

5. CONCLUSION

Hamitabat CCPP is the first combined cycle plant of Turkey, and it is renovated in 2017. The natural gas fueled plant has an installed power of 1220 MW, and it has a key role in the energy security of the country. In this study, the energy and exergy analysis of the Hamitabat CCPP is performed for one unit of the plant by using the operating data. Global and component-based performance analysis of the plant is carried out to determine the power production or consumption, heat loss or gain, exergy destruction rate, exergy efficiency and improvement potential of components and the thermal and exergy efficiencies of the whole plant. In addition, parametric analyses were made to examine the impacts of condenser pressure, inlet temperature of high- and

intermediate-pressure steam turbines and the pressure of high-pressure steam turbine on the performance of the plant. The findings of the study are summarized as follows:

- Hamitabat CCPP has a thermal efficiency of 59.70% and an exergy efficiency of 58.52%. The 520 million € renovation project, completed in 2017, has increased the thermal and exergy efficiencies of the plant by 13.70% and 13.52%, respectively.
- Combustion chamber has the largest exergy destruction rate of 307.389 MW which corresponds to 77.61% of plant's total exergy destruction rate. The component is followed by the heat recovery steam generator and compressor having irreversibility rates of 25.287 MW and 22.785 MW, respectively.
- Preventing heat loss from the combustion chamber can significantly improve the performance of the CCPP. In the limiting case of an adiabatic combustion chamber, the thermal and exergy efficiencies can be increased by 3.88% and 3.80%, respectively.
- The thermal and exergy efficiencies of the plant can be improved by increasing the inlet temperatures of high- and intermediate-pressure turbines, and decreasing the pressures of condenser and high-pressure turbine.

The analysis presented in this study is useful in assessing the outcome of the renovation project, and it provides critical information and suggestions to the engineers and operators of the power plant for improving the performance characteristics of the plant. Thermal efficiency and environmental performance of the Hamitabat CCPP can be further enhanced by precooling the air at the compressor inlet and utilizing a supplementary firing system. Future work needs to be performed to examine the impact of these approaches and the model presented in this paper can constitute the base for modeling. Also, such a performance improvement analysis can be carried out in exergoeconomic and exergoenvironmental frameworks in order to include economic and greenhouse gas emission factors.

NOMENCLATURE

C	Compressor
CC	Combustion chamber
CCCP	Cooling cycle circulation pump
CCPP	Combined cycle power plant
COND	Condenser
CP	Condenser pump

CPR	Compressor pressure ratio
CT	Cooling turbine
D	Drum
FWP	Feedwater pump
G	Generator
GC	Gland condenser
GT	Gas turbine
HP ECO	High-pressure economizer
HP SH	High-pressure superheater
HPST	High-pressure steam turbine
HRSG	Heat recovery steam generator
HT	Hydraulic turbine
IP ECO	Intermediate-pressure economizer
IP RH	Intermediate-pressure reheater
IP SH	Intermediate-pressure superheater
IPST	Intermediate-pressure steam turbine
JANAF	Joint Army Navy Air Force
LP SH	Low-pressure superheater
LPST	Low-pressure steam türbine
NGPH	Natural gas preheater
PH	Preheater
PU	Polishing unit
ST	Steam turbines
TIT	Turbine inlet temperature

DECLARATION OF ETHICAL STANDARDS

The authors of the paper submitted declare that nothing which is necessary for achieving the paper requires ethical committee and/or legal-special permissions.

CONTRIBUTION OF THE AUTHORS

Göksel Topal: Collected data, Modelling, Performed the analyses, Writing - original draft.

Tayfun Tanbay: Literature review, Modelling Interpretation of the results, Writing - review & editing, Supervision.

CONFLICT OF INTEREST

There is no conflict of interest in this study.

REFERENCES

[1] Tran BL, Chen CC, Tseng WC. Causality between energy consumption and economic growth in the presence of GDP threshold effect: Evidence from OECD countries. Energy 2022; 251: 123902.

[2] Osicka J, Cernoch F. European energy politics after Ukraine: The road ahead. Energy Research & Social Science 2022; 91: 102757.

[3] Eurostat. Fossil fuels led in electricity generation in 2021. https://ec.europa.eu/eurostat/web/products-eurostat-news/-/ddn-20220630-1. Accessed on 24/02/2023.

[4] Aliyu M, AlQudaihi AB, Said SA, Habib MA. Energy, exergy and parametric analysis of a combined cycle power plant. Thermal Science and Engineering Progress 2020; 15: 100450.

[5] Ibrahim TK, Mohammed MK, Awad OI, Rahman MM, Majafi G, Basrawi F, Abdalla AN, Basrawi F, Mamat R. The optimum performance of the combined cycle power plant: A comprehensive review. Renewable and Sustainable Energy Reviews 2017; 79: 459-474.

[6] Ibrahim TK, Mohammed MK, Awad OI, Abdalla AN, Basrawi F, Mohammed MN, Najafi G, Mamat R. A comprehensive review on the exergy analysis of combined cycle power plants. Renewable and Sustainable Energy Reviews 2018; 90: 835-850.

[7] Garcia SI, Garcia RF, Carril JC, Garcia DI. Critical review of the first-law efficiency in different power combined cycle architectures. Energy Conversion and Management 2017; 148: 844-859.

[8] Facchini B, Fiaschi D, Manfrida G. Exergy analysis of combined cycles using latest generation gas turbines. Journal of Engineering for Gas Turbines and Power 2000; 122: 233-238.

[9] Sue DC, Chuang CC. Engineering design and exergy analyses for combustion gas turbine based power generation system. Energy 2004; 29: 1183-1205.

[10] Ertesvag IS, Kvamsdal HM, Bolland O. Exergy analysis of a gas-turbine combined-cycle power plant with precombustion CO_2 capture. Energy 2005; 30: 5-39.

[11] Arrieta FRP, Lora EES. Influence of ambient temperature on combined-cycle power-plant performance. Applied Energy 2005; 80: 261-272.

[12] Cziesla F, Tsatsaronis G, Gao Z. Avoidable thermodynamic inefficiencies and costs in an externally fired combined cycle power plant. Energy 2006; 31: 1472-1489.

[13] Sanjay Y, Singh O, Prasad BN. Energy and exergy analysis of steam cooled reheat gas-steam combined cycle. Applied Thermal Engineering 2007; 27: 2779-2790.
[14] Sanjay Y, Prasad BN. Energy and exergy analysis of intercooled combustion-turbine based combined cycle power plant. Energy 2013; 59: 277-284.
[15] Bassily AM. Modeling, numerical optimization, and irreversibility reduction of a triple-pressure reheat combined cycle. Energy 2007; 32: 778-794.
[16] Pattanayak L, Sahu JN, Mohanty P. Combined cycle power plant performance evaluation using exergy and energy analysis. Environmental Progress & Sustainable Energy 2017; 36: 1180-1186.
[17] Koch C, Cziesla F, Tsatsaronis G. Optimization of combined cycle power plants using evolutionary algorithms. Chemical Engineering and Processing 2007; 46: 1151-1159.
[18] Ameri M, Ahmadi P, Khanmohammadi S. Exergy analysis of a 420 MW combined cycle power plant. International Journal of Energy Research 2008; 32: 175-183.
[19] Ahmadi P, Dincer I, Rosen MA. Exergy, exergoeconomic and environmental analyses and evolutionary algorithm based multi-objective optimization of combined cycle power plants. Energy 2011; 36: 5886-5898.
[20] Ahmadi P, Dincer I. Thermodynamic analysis and thermoeconomic optimization of a dual pressure combined cycle power plant with a supplementary firing unit. Energy Conversion and Management 2011; 52: 2296-2308.
[21] Petrakopoulou F, Tsatsaronis G, Morosuk T, Carassai A. Conventional and advanced exergetic analyses applied to a combined cycle power plant. Energy 2012; 41: 146-152.
[22] Mansouri MT, Ahmadi P, Kaviri AG, Jaafar MNM. Exergetic and economic evaluation of the effect of HRSG configurations on the performance of combined cycle power plants. Energy Conversion and Management 2012; 58: 47-58.
[23] Kaviri AG, Jaafar MNM, Lazim TM, Barzegaravval H. Exergoenvironmental optimization of Heat Recovery Steam Generators in combined cycle power plant through energy and exergy analysis. Energy Conversion and Management 2013; 67: 27-33.
[24] Soltani S, Mahmoudi SMS, Yari M, Rosen MA. Thermodynamic analyses of an externally fired gas turbine combined cycle integrated with a biomass gasification plant. Energy Conversion and Management 2013; 70: 107-115.
[25] Açıkkalp E, Aras H, Hepbasli A. Advanced exergoeconomic analysis of an electricity-generating facility that operates with natural gas. Energy Conversion and Management 2014; 78: 452-460.

[26] Boyaghchi FA, Molaie H. Sensitivity analysis of exergy destruction in a real combined cycle power plant based on advanced exergy method. Energy Conversion and Management 2015; 99: 374-386.
[27] Boyaghchi FA, Molaie H. Advanced exergy and environmental analyses and multi objective optimization of a real combined cycle power plant with supplementary firing using evolutionary algorithm. Energy 2015; 93: 2267-2279.
[28] Vandani AMK, Joda F, Boozarjomehry RB. Exergic, economic and environmental impacts of natural gas and diesel in operation of combined cycle power plants. Energy Conversion and Management 2016; 109: 103-112.
[29] Sahin AZ, Al-Sharafi A, Yilbas BS, Khaliq A. Overall performance assessment of a combined cycle power plant: An exergo-economic analysis. Energy Conversion and Management 2016; 116: 91-100.
[30] Blumberg T, Assar M, Morosuk T, Tsatsaronis G. Comparative exergoeconomic evaluation of the latest generation of combined-cycle power plants. Energy Conversion and Management 2017; 153: 616-626.
[31] Hosseini SE, Barzegaravval H, Ganjehkaviri A, Wahid MA, Jaafar MNM. Modelling and exergoeconomic-environmental analysis of combined cycle power generation system using flameless burner for steam generation. Energy Conversion and Management 2017; 135: 362-372.
[32] Ersayin E, Ozgener L. Performance analysis of combined cycle power plants: A case study. Renewable and Sustainable Energy Reviews 2015; 43: 832-842.
[33] Abuelnuor AAA, Saqr KM, Mohieldein SAA, Dafallah KA, Abdullah MM, Nogoud YAM. Exergy analysis of Garri "2" 180MW combined cycle power plant. Renewable and Sustainable Energy Reviews 2017; 79: 960-969.
[34] Ali MS, Shafique QN, Kumar D, Kumar S, Kumar S. Energy and exergy analysis of a 747-MW combined cycle power plant Guddu. International Journal of Ambient Energy 2020; 41: 1495-1504.
[35] Jamnani MB, Kardgar A. Energy-exergy performance assessment with optimization guidance for the components of the 396-MW combined-cycle power plant. Energy Science & Engineering 2020; 8: 3561-3574.
[36] Pinto GM, Coronado CJR, de Souza TUZ, Santos EMD. Exergy analysis of a natural gas combined cycle power plant: a case study. International Journal of Exergy 2022; 37: 159-180.

[37] Altarawneh OR, Alsarayreh AA, Al-Falahat AM, Al-Kheetan MJ, Alrwashdeh SS. Energy and exergy analyses for a combined cycle power plant in Jordan. Case Studies in Thermal Engineering 2022; 31: 101852.

[38] Pattanayak L, Padhi BN. Thermodynamic simulation and economic analysis of combined cycle with inlet air cooling and fuel pre-heating: Performance enhancement and emission reduction. Energy Conversion and Management 2022; 267: 115884.

[39] Shireef LT, Ibrahim TK. Influence of operating parameters on the performance of combined cycle based on exergy analysis. Case Studies in Thermal Engineering 2022; 40: 102506.

[40] Republic of Türkiye Ministry of Energy and Natural Resources. Electricity. https://enerji.gov.tr/bilgi-merkezi-enerji-elektrik (in Turkish) accessed on 15/07/2023.

[41] EPDK. Turkish Natural Gas Market Report 2021. Energy Market Regulatory Authority: Ankara, 2022.

[42] Cihan A, Hacıhafızoğlu O, Kahveci K. Energy-exergy analysis and modernization suggestions for a combined-cycle power plant. International Journal of Energy Research 2006; 30: 115-126.

[43] Chase MW. NIST-JANAF Thermochemical Tables 2 Volume-Set, Journal of Physical and Chemical Reference Data Monographs. American Institute of Physics, College Park, MD, 1998.

[44] Pamidimukkala KM, Rogers D, Skinner GB. Ideal gas thermodynamic properties of CH_3, CD_3, CD_4, C_2D_2, C_2D_4, C_2D_6, C_2H_6, $CH_3N_2CH_3$, and $CD_3N_2CD_3$. Journal of Physical and Chemical Reference Data 1982; 11: 83-99.

[45] Chao J, Wilhoit RC, Zwolinski BJ. Ideal gas thermodynamic properties of Ethane and Propane. Journal of Physical and Chemical Reference Data 1973; 2: 427-437.

[46] Çengel YA, Boles MA. Thermodynamics: An Engineering Approach, 8th ed. McGraw-Hill, USA, 2015.

[47] Van Gool W. Energy policy: fairy tales and factualities, in: Innovation and Technology-Strategies and Policies 1997, Springer, 93-105.